Published in final edited form as:
Pharmacology. 2016 ; 98(5-6): 251–260. doi:10.1159/000448007.

Alpha-Smooth Muscle Actin mRNA and Protein Are Increased in Isolated Brain Vessel Extracts of Alzheimer Mice

Bianca Hutter-Schmid and **Christian Humpel**
Department of Psychiatry, Psychotherapy and Psychosomatics, Laboratory of Psychiatry and Experimental Alzheimer's Research, Medical University of Innsbruck, Innsbruck, Austria

Abstract

Alzheimer’s disease (AD) is a severe neurodegenerative disorder of the brain, characterized by extracellular beta-amyloid plaques, intracellular tau pathology, neurodegeneration and inflammation. There is clear evidence that the blood-brain barrier is damaged in AD and that vessel function is impaired. Alpha-smooth muscle actin (αSMA) is a prominent protein expressed on brain vessels, especially in cells located closer to the arteriole end of the capillaries, which possibly influences the blood vessel contraction. The aim of the present study was to observe αSMA protein and mRNA expression in isolated brain vessel extracts and cortex in an Alzheimer mouse model with strong beta-amyloid plaque deposition. Our data revealed a prominent expression of αSMA protein in isolated brain vessel extracts of AD mice by Western Blot analysis. Immunostainings showed that these vessels were associated with beta-amyloid plaques. Quantitative real-time PCR analysis confirmed this increase at the mRNA expression level, and showed a significant increase of TGFβ1 mRNA expression in AD mice. In situ hybridization demonstrated a strong expression pattern of αSMA mRNA in the whole cortex and hippocampus. In conclusion, our data provide evidence that αSMA protein and mRNA are enhanced in vessels in an AD mouse model, possibly counteracting vessel malfunction in AD.

Keywords

brain vessels; Alzheimer’s disease; Alpha-smooth muscle actin; transforming growth factor–β1

Introduction

Alzheimer’s disease (AD) is the most frequent cause of dementia worldwide and is characterized by beta-amyloid (Aβ) depositions in brain (plaques) and vessels (cerebral amyloid angiopathy, CAA), formation of neurofibrillary tangles (the abnormally aggregated and hyper-phosphorylated form of tau), cerebrovascular dysfunction, cell death of cholinergic neurons, microglial activation and inflammation [1–3]. The reasons for developing AD are still not known, however, it is known that vascular risk factors contribute to cognitive decline [4–7]. Several cerebrovascular abnormalities have been described in the pathogenesis of AD, including basement membrane thickening, loss of pericytes, damage of endothelial cells, brain vessels expressing inflammatory markers, anthropic vessels, reduced glucose transport across the blood-brain barrier (BBB), changes in vessel diameter, accumulation of e.g. collagen in atheriosclerotic plaques [8].

Europe PMC Funders Author Manuscripts

There is clear evidence that brain vessels are damaged in AD and that the blood flow is decreased. However, so far it is still not known if these pathological dysfunctions are a primary event in the development of AD or if the vessel pathology is caused secondary by plaque depositions. Brain vessels are composed of endothelial cells and pericytes and play an important role in in the regulation of blood flow, maintenance and formation of the BBB and in the regulation of immune cell entry to the brain [1–2, 9]. Alpha-smooth muscle actin (αSMA) is a cytoskeletal protein and highly expressed in brain vessels, especially in postcapillary arterioles, playing an important role in vessel constriction [10–12]. These vessel cells are possibly involved in the regulation of blood flow due to their expression of αSMA [13,14]. However, so far the regulation of αSMA in vessels of AD brains is not fully understood, because there is conflicting results in human brains.

Thus, the aim of the present study is to investigate the αSMA protein and mRNA expression in an AD mouse model where amyloid precursor protein (APP) is overexpressed with a Swedish, Dutch and Iowa triple-mutation.

Material and Methods

Animals

Wildtype (WT, C57BL6N) and transgenic APPSweDI (Tg-SweDI; expressing amyloid precursor protein (APP) harboring the Swedish K670N/M671L, Dutch E693Q, and Iowa D694N mutations; C57BL/6-Tg(Thy1-APPSwDutIowa) BWevn/Mmjax) mice were purchased from The Jackson Laboratory and housed at the Innsbruck Medical University animal facility providing open access to food and water under 12 h/12 h light–dark cycles. All experiments were approved by the Austrian Ministry of Science and Research and conformed to the Austrian guidelines on animal welfare and experimentation.

Immunohistochemistry

Anaesthetized (Ketamin 100 mg/kg/ Xylazine 10 mg/kg) 12 month old wildtype and transgenic mice were transcardially perfused with 20 ml phosphate-buffered saline (PBS) to verify that the vessels are free of blood, then the brains were collected and fresh frozen in a CO_2 stream. Brains were cut into coronal sections of 40 μm with a cryostat (Leica CM 1950) and placed onto gelatine-coated glass slides. Immunohistochemistry was performed as described in detail [15–16]. In brief, brain sections were washed in PBS and subsequently fixed with 4% paraformaldehyde for 30 min. Then, fixed sections were again washed with PBS and incubated in PBS/0.1% Triton (T-PBS) for 30 min at room temperature (RT) while shaking. To quench endogenous peroxidase, sections were treated with PBS/1%H_2O_2/5% methanol. After incubation, the sections were then blocked in T-PBS/20% horse serum (GIBCO Invitrogen)/0.2% bovine serum albumin (BSA, SERVA) for 30 min at RT while shaking. Following blocking, brain sections were incubated with primary antibody (alpha-smooth muscle actin, 1:1000, Novus Biologicals NB300-978) in T-PBS/0.2% BSA for 2 days at 4°C. The sections were then washed and incubated with fluorescent Alexa-488 (Invitrogen-Life Tech, Vienna, Austria) secondary antibody in T-PBS/0.2% BSA for 1 h at RT while shaking. Some sections were counterstained with nuclear DAPI (0.1 μg/ml, 1hr

4°C) or with Lectin (1:100, 1hr, 4°C). Finally, the sections were washed with PBS and cover-slipped with Mowiol 4-88 (Roth, Austria).

Some brain sections were processed using the chromogenic substrate diaminobenzidine (DAB, Sigma) as described earlier [17]. Briefly, after incubation with the primary antibodies PDGFRβ (clone Y92, 1:3000, Novus Biologicals NB110-57343), alpha-smooth muscle actin (1:1000, Novus Biologicals NB300-978; 1:250, abcam, ab119952) or beta-amyloid (Aß, 1-16, 6E10 monoclonal, Covance) brain sections were washed and incubated with the corresponding biotinylated secondary antibody (1:200, Vector Laboratories) in T-PBS/0.2% BSA for 1 h at RT while shaking. Following secondary antibody incubation, sections were rinsed with PBS and incubated in avidin–biotin complex solution (Elite ABC kit, Vector Laboratories) for 1 h at RT, while shaking. Finally, the sections were washed with 50 mM Tris-buffered saline (TBS) and then incubated in 0.5 mg/ml 3,3′-diaminobenzidine/TBS/ 0.003% H_2O_2 at RT in the dark until a signal was detected. Once DAB staining was visible, the reaction was stopped by adding TBS to the sections. The brain sections were rinsed with TBS, and dehydrated in an ascending ethanol series, cleared in butylacetate, and cover slipped with Entellan® (Merck, Darmstadt, Germany) whereas primary pericytes were directly cover-slipped with Mowiol 4-88 (Roth, Austria).

Some sections were processed for chromogenic co-localization as described by us [17]. In brief, brain sections were first prepared for αSMA immunohistochemistry and stained with the chromogenic substrate DAB giving a brown color. Sections were then washed in PBS, blocked with the avidin/biotin blocking kit (Vector SP-2001), then processed for Aβ immunohistochemistry and finally stained with Vector SG substrate (SK-470) giving a grey color. Control experiments for all antibodies were conducted by omitting the primary antibody. Staining was visualized with an Olympus BX61 fluorescence microscope and pictures captured with Openlab software.

Isolation of brain vessel extracts

Brain vessel extracts which include endothelial cells as well as vessel-associated cells like pericytes and vascular smooth muscle cells (brain vessel extracts), were isolated from C57BL/6N as well as Tg-SweDI mouse brains (age 12 month) as reported previously [18]. In brief, mice were euthanized, brains extracted and subsequently placed in Optimem medium (Gibco). Then, the olfactory bulb as well as medulla and cerebellum were removed and the remaining brain was minced into 1 mm^3 pieces with a razor blade. Afterwards, the minced brain tissue was washed with Optimem and centrifuged in a Hettich centrifuge Rotina 46R at 1000xg for 5 min at room temperature (RT). Subsequently, the washed tissue was re-suspended in Optimem and homogenized by using a glass-potter (20 times). After another centrifugation step at 1000xg for 10 min at RT, the homogenized cells were mixed with 20 ml of 25 % bovine serum albumine (BSA, SERVA) in Optimem and centrifuged at 3400xg for 20 min at RT without using the brake. After centrifugation, the lipid layer on top of the vial was removed and the cell pellet was subsequently washed in PBS. Finally, the isolated brain vessels were dissolved in PBS containing a protease inhibitor cocktail (P-8340, Sigma), homogenized using an ultrasonic device (Hielscher Ultrasonic Processor,

Germany) and centrifuged at 14.000xg for 10 min at 4°C. The extracts were stored at -80°C until use for Western Blots.

Western Blot Analysis

Western blot analysis was performed as previously described by us [16]. Twenty µl of the cell/vessel extracts were loaded onto 10% Bis-Tris SDS-polyacrylamide gels (Thermo Fisher Scientific), separated for 35 min at 200 V and finally electro-transferred to nylon-PVDF Immobilon-PSQ membranes for 90 min at 30 V in 20% methanol blotting buffer. Briefly, blots were blocked for 30 min in blocking buffer, incubated with primary antibodies against PDGFRβ clone Y92 (C-terminal, amino acid (aa)1050-1150) (1:3000, Novus Biologicals NB110-57343), alpha-smooth muscle actin (1:1000, abcam ab119952), actin (1:1000, Sigma A2066) or laminin (1:500, Sigma) at 4°C overnight, washed, and then incubated in alkaline phosphatase conjugated anti-rabbit IgG or anti-mouse IgG for 30 min. After washing, bound antibodies were detected using an enhanced chemiluminescence (ECL) system and visualized by using a cooled CCD camera (SearchLight; Thermo Fisher Scientific).

In situ hybridization

In situ hybridization was performed as described [19]. Mice (12-month-old wildtype and Tg-SweDI) were decapitated and the brains frozen under a CO_2 stream, sectioned (14 µm) with a cryostat (Leica) and thawed onto slides (ProbeOn™ slides, Fisher Biotech, Austria). Oligonucleotides (5 pmol) specific for αSMA (αSMA-antisense: 5´-tca-ggc-agt-tcg-tag-ctc-ttc-tcc-agg-gag-3´; αSMA-sense: 5´-ctc-cct-gga-gaa-gag-cta-cga-act-gcc-tga-3´; see also [20] were labeled at the 3´end with [α-^{35}S]dATP using terminal deoxyribonucleotidyl transferase (Roche, Austria) and purified by using a Nucleotide Removal Kit (Qiagen). Brain sections were hybridized overnight at 42°C in a humidified chamber with 100 µl per section of the hybridization solution (50% formamide, 4xSSC, 0.02% polyvinylpyrrolidone, 0.02% Ficoll, 0.02% bovine serum albumin, 10% dextrane sulfate, 0.5 mg/ml sheared salmon sperm DNA, 1% sarcosyl (N-lauroyl sarcosine), 0.02M $NaPO_4$ (pH 7.0), 50 mM dithiothreitol) containing 1x10^7 CPM/ml probe. Sections were subsequently rinsed, washed four times (15 min each) in 1xSSC (saline sodium citrate) at 54°C, cooled to room temperature, dehydrated through 70%, 90% and 99.9% ethanol and air-dried. Sections were dipped in Kodak NTB photo emulsion, exposed for 5 weeks at -20°C, developed, fixed and subsequently counterstained with DAPI (0.1 µg/ml, 2hr RT) and thioflavin S (1.6 µg/ml 2hr RT, Sigma T1892). Finally, the sections were mounted with Mowiol 4-88 (Roth, Austria) and stored in the dark at 4°C until analysis. As a control, selected sections were incubated with 500x excess of unlabeled antisense-oligonucleotides.

RNA Isolation and Quantitative TaqMan-PCR

Quantitative RT-PCR was performed as described [19]. In brief, mice (Wt and Tg mice 12 months old) were euthanized, brain cortices were transferred to 600 µl of Buffer RLT (RNeasy Mini Kit; Qiagen) and homogenized utilizing an ultrasonic device (Hielscher Ultrasonic Processor, Germany) and further disrupted by using QIAshredder columns (Qiagen). Total RNA was extracted with the RNeasy Mini Kit (Qiagen). RNA concentrations were determined photometrically using BioPhotometer 6131 (Eppendorf).

Reverse transcription was performed on 250 ng of total RNA using the Omniscript Reverse Transciptase Kit (Qiagen), random hexamer primers (Promega) and RNAse Inhibitor (Sigma). The reverse transcription mix was incubated for 60 min at 37 °C. The relative expression of *Acta2* (αSMA), *Tgfβ1* and *Pdgfrβ* mRNA was obtained by TaqMan quantitative PCR (qRT-PCR) using a standard curve method based on PCR products of known concentration in combination with normalization using the house keeping gene *Glycerinaldehyd-3-phosphat-dehydrogenase* (*Gapdh*). TaqMan gene expression assays specific for the genes *Acta2*, *Tgfβ1* and *Pdgfrβ* designed to span exon-exon boundaries, were purchased from Applied Biosystems. The following assays (Applied Biosystems) were used [gene symbol, assay ID]: *Acta2* (αSMA), Mm01204962_gH; *Tgfβ1*, Mm01178820_m1 and *Pdgfrβ*, Mm00435547_m1. The endogenous control gene included was [gene symbol, assay ID] glyceraldehyde-3-phosphate dehydrogenase (*Gapdh*), Mm99999915_g1. qRT-PCR (50 cycles) was performed in quadruplicates, using 1 μl total RNA equivalents of cDNA and the specific TaqMan gene expression assay for each 20 μl reaction in TaqMan Universal PCR Master Mix (Applied Biosystems). Analysis was performed utilizing the QuantStudio 6 (Applied Biosystems). The Ct values for each gene expression assay were recorded for each individual preparation. To allow a direct comparison between expression levels in cortices from different mice, we normalized all experiments to *Gapdh*. Finally, normalized molecule numbers were calculated for each gene from their respective standard curve.

Quantification

Quantification of Aβ-plaques, αSMA-positive as well as PDGFRβ-positive vessels was performed by capturing images with an Olympus BX61 microscope using Openlab imaging software and acquired under the same exposure settings. For quantification, 4-6 brain sections per animal (wildtype (C57BL/6) and transgenic (Tg-SweDI) mice) were evaluated for cortical staining patterns using 10x magnification. The number of Aβ-positive plaques were evaluated and quantified by utilizing ImageJ software (NIH). Images were normalized to the same threshold levels and converted into binary formats. Plaque burden was quantified by counting the plaques per field [1087x817 μm^2], whereas every particle with a size between 5 μm and <40 μm was defined as a plaque. αSMA-positive vessels were quantified in size (cut off 200 μm) and density (optical density). The PDGFRβ-positive mouse brain vessels were counted in a 6 × 6 grid**.** Briefly, a digital picture was taken under the microscope at a 10x magnification. The digital picture was overlaid with a 6 × 6 grid using Photoshop (Adobe Photoshop CS6) and the number of all vessels crossing all lines was counted. Western Blots were normalized to laminin expression and quantified by measuring the optical density.

Data Analysis and Statistics

All data are reported as mean ± SEM. Differences between mean values were determined using one-way ANOVA followed by a Fisher least significant difference post hoc test or students T-test. Statistical results were considered significant at $p < 0.05$ (*p<0.05; **p<0.01; ***p<0.001).

Results

Cellular expression of Aβ, αSMA and PDGFRβ protein

A high number of Aβ plaques was found throughout the cortex of 12-month-old Tg-SweDI mice, whereas no Aβ staining was seen in the cortex of 12-month-old C57BL/6 wildtype mice (Fig.1 A-D). Both wildtype C57BL/6 as well as Tg-SweDI mice showed prominent αSMA staining around brain vessels within cortices (Fig.1 E-F) but the vessel density did not differ between wildtype and Tg-SweDI mice (Fig.1 H). In addition, a larger vessel size was observed in the cortices of Tg-SweDI mice compared to wildtype C57BL/6 mice (Fig.1 H). Both Tg-SweDI as well as C57BL/6 wildtype mice showed a pronounced PDGFRβ staining around brain vessels in the cortices, however, a slight not significant decrease of PDGFRβ expression was found in the cortex of Tg-SweDI mice compared to C57BL/6 wildtype mice (Fig.1 I-J, L). Omitting the primary antibodies showed only background stainings (Fig.1 C, G, K). Co-localization studies showed that αSMA positive staining was observed in lectin positive cortex vessel extracts (Fig.2 A-D). Co-expression of αSMA with Aβ in 12-month-old Tg-SweDI mouse brains showed several αSMA-positive brain vessels clearly associated with Aβ plaques (Fig. 2 E).

αSMA protein in isolated cortex vessel extracts

Western Blot analysis indicated a significant increase of αSMA protein expression in cortex vessel extracts isolated from 12-month-old Tg-SweDI mice compared to C57BL/6 wildtype mice (Fig.3 A, B). Actin showed a similar staining pattern as αSMA (Fig. 3 A). Laminin served as a loading control (Fig. 3 A).

αSMA mRNA expression and qRT-PCR

In situ hybridization for αSMA mRNA showed a strong mRNA expression in the whole cortex and hippocampus of C57BL/6 wildtype and Tg-SweDI mice as visualized in darkfield microscopy (Fig.4 B-C). No signal was obtained in sections incubated with sense oligonucleotides (Fig. 4A) or sections with 500-fold non-labelled oligonucleotides excess (Fig. 4D). Co-labeling with nuclear DAPI shows the black silver grains in the vicinity of cell nuclei in brightfield microscopy (Fig. 4E). Co-staining with Thioflavin-S demonstrated αSMA mRNA expressing cells around plaques (Fig. 4F). Quantitative real-time PCR analysis showed a significantly increased αSMA mRNA expression as well as TGFβ1 mRNA expression in the cortex of 12-month old transgenic Tg-SweDI mice compared to C57BL/6 wildtype mice (Fig.5). The PDGFRβ mRNA expression in transgenic Tg-SweDI mice was not affected (Fig. 5).

Discussion

In the present study we report on the expression of αSMA protein and mRNA in an AD mouse model where amyloid precursor protein (APP) is overexpressed with a Swedish, Dutch and Iowa triple-mutation.

Alpha-smooth muscle actin

Mammalian alpha-smooth muscle actin is a cytoskeletal protein, expressed from the *Acta2* gene and translated as 6 different isoforms: cardiac and skeletal α-actin, visceral and vascular α- and γ-smooth muscle actin and β- and γ-cytoplasmic actin [21, 22]. Interestingly, these actin isoforms differ from each other by less than 5% of their amino acid sequence [22–24]. In general, actin is responsible for several essential cell functions including e.g. transcriptional regulation, cell migration and division, chromatin remodeling or tight junction formation [22] but each isoform has a specialized function [25–27]. Interestingly, αSMA knockout mice are viable but have severe defects in blood pressure regulation and vascular contractility [26]. In the present study, we used two different αSMA antibodies, one from Novus and one from Abcam. Both antibodies recognized a protein of 42 kDa, the same size as actin. Thus, for Western Blot analysis we used laminin as a loading control. Although we cannot completely exclude cross-binding of our αSMA antibodies with other isoforms, we can selectivity verify αSMA^{+}like immunoreactivity on cellular vessel stainings and in isolated vessel extracts. In fact, all these stainings gave a clear convincing pattern for αSMA expression in brain vessel associated cells. For in situ hybridization we used selective oligonucleotides, the same as reported by Ghassemifar et al. [20], however, cross-reactivity cannot be excluded due to the high sequence homology to actin. In fact, the mRNA expression pattern points to a rather homogenous high expression in several cells in the cortex including neurons in the hippocampal formation. Although we cannot exclude a discrepancy between protein and mRNA expression, a differential expression pattern or reduced sensitivity of the immunostaining may result in this differential expression pattern. Thus, to exclude such unspecificity, high purified vessel preparations were used for Western Blot analysis which, indeed, showed a marked specific upregulation of αSMA in the AD mouse model.

Expression of αSMA in the brain

The expression of αSMA in the brain starts during vascular development and is predominantly found in adult vascular smooth muscle cells [28]. Further, a transient expression of αSMA is also observed in non-muscle cells including pericytes and fibroblasts [21, 29, 30]. In contrast, β- as well as γ-non-muscle actins are ubiquitously expressed [29]. Interestingly, during embryonic and postnatal development some astrocytes with a myofibroblastic feature also express αSMA, but its expression decreases during CNS maturation [31–33]. Moreover, the expression of several actin isoforms is found to be upregulated within astrocytes during CNS injury [34–36]. Further, Moreels et al. [37] observed an expression of αSMA in reactive astrocytes in multiple sclerosis lesions. There is also clear evidence that hypertension influence the αSMA gene expression in contractile cells at the brain microvasculature [38]. As discussed previously, our data are in full agreement and show specific αSMA protein expression in adult brain vessel extracts, although we cannot yet define the exact cellular localization. Regarding αSMA mRNA expression, we show a homogenous expression in nearly all cells in the whole cortex and hippocampal formation. It seems likely that there was strong crossreactivity with actin mRNA due to its high homology. This may also explain why we could not confirm the qRT-PCR data at the cellular level. Further, co-localization was not possible when using ^{35}S-radioactive labelled oligonucleotides.

αSMA in Alzheimer's disease

Microvascular dysfunction, neurovascular aberrations and malfunctions of the BBB are major hallmarks in AD [39–41]. There seems to be strong evidence that αSMA expression is markedly decreased in cerebral blood vessels of postmortem AD patients compared to healthy age-matched controls [42, 43]. This severity of loss of αSMA in AD patients was highly dependent on the apolipoprotein E4 genotype [42]. However, the same group published some years ago that αSMA is increased in non-demented patients with frequent senile plaques [44]. While this seems to be conflicting results, there is now evidence that the progressing Aβ-associated angiopathy as well as the extent of cerebrovascular damage may play an essential role. To our best knowledge we report for the first time of an increased expression of αSMA protein and mRNA in a transgenic AD mouse model. This increase of αSMA was also confirmed at the mRNA expression level by qRT-PCR, while no changes in PDGFRβ mRNA expression were observed. Our APP_SweDI mouse model only partially reflects the full AD pathology because no tau pathology and only limited angiopathy is present. Further, the apolipoprotein E effect cannot be verified. Thus, our data suggest that the extensive plaque load going along with vascular impairment causes a marked upregulation of αSMA in isolated vessel extracts. It seems likely that this enhanced expression may be caused by counteracting the dysfunctional blood flow. Further, the brain vessels and especially the pericytes may undergo a strong regenerative plasticity after degenerative insults. It is known that αSMA knock out mice can express skeletel actin in vascular smooth muscle cells in the abscence of αSMA [26]. Moreover, pericytes display stem cell activity after different insults, and can differentiate into other cells, such as e.g. glial cells [45]. In summary, the increased vessel αSMA protein in the AD mouse model may reflect a pathological sign during the progression of the AD pathology but is highly dependent on the Aβ pathology.

Role of TGFβ1

TGFβ1 is highly activated during the AD pathology [46–51] and TGFβ1 mediated inflammation modulates deposition of cerebral plaques and CAA and age-dependent cognitive decline [52, 53, 54–57]. It is well known that brain microvessels from patients suffering from AD secrete enhanced levels of inflammatory mediators including TGFβ1 [56]. Moreover, increased levels of TGFβ1 were also observed in cerebrospinal fluid and within Aβ plaques [50, 54, 55, 58, 59]. Furthermore, enhanced TGFβ1 may modulate the microglia response, leading to an enhanced microglia-mediated Aβ degradation [47, 60]. Using qRT-PCR, we demonstrate that TGFβ1 mRNA expression was significanly enhanced in transgenic Alzheimer mice, supporting the role of TGFβ1 in the AD pathology, although we cannot directly proof yet that TGFβ1 affects αSMA expression in vessels.

Conclusion

In conclusion, our data show that αSMA protein and mRNA are increased in isolated brain vessels in an AD mouse model. These transgenic AD mice showed also a strong increase of TGFβ1 mRNA expression. Thus, it is concluded that αSMA is enhanced in impaired AD vessels to possibly counteract vessel malfunction in AD.

Europe PMC Funders Author Manuscripts

Acknowledgements

This study has been supported by the Austrian Science Funds (P24734-B24). We thank Karin Albrecht for excellent technical work with Western Blot analyses. We thank members of the MUI qRT-PCR core unit for help with expression assays.

References

1. Sagare AP, Bell RD, Zhao Z, Ma Q, Winkler EA, Ramanathan A, Zlokovic BV. Pericyte Loss Influences Alzheimer- like Neurodegeneration in mice. Nat Commun. 2013; 4:2932–2946. [PubMed: 24336108]
2. Winkler EA, Sagare AP, Zlokovic BV. The pericyte: a forgotten cell type with important implications for Alzheimer's disease? Brain Pathol. 2014; 24:371–386. [PubMed: 24946075]
3. Querfurth HW, La Ferla FM. Alzheimer´s Disease. N Engl J Med. 2010; 28:329–344.
4. Horstman LL, Jy W, Ahn YS, Zivadinov R, Maghzi AH, Etemadifar M, Steven Alexander J, Minagar A. Role of platelets in neuroinflammation a wide-angle perspective. J Neuroinfallmation. 2010; 7:10.
5. Humpel C. Chronic mild cerebrovascular dysfunction as a cause for Alzheimers disease. Exp Gerontol. 2011; 46:225–232. [PubMed: 21112383]
6. Iadecola C. Neurovascular regulation in the normal brain and in Alzheimer's disease. Nat Rev Neurosci. 2004; 5:347–360. [PubMed: 15100718]
7. De la Torre JC. Alzheimer´s disease as a vascular disorder. Stroke. 2000; 33:1152–1162.
8. Farkas E, Luiten PG. Cerebral microvascular pathology in aging and Alzherimer's disease. Prog Neurobiol. 2001; 64:575–611. [PubMed: 11311463]
9. Dalkara T, Gursoy-Ozdemir Y, Yemisci M. Brain microvascular pericytes in health and disease. Acta Neuropathol. 2011; 122:1–9. [PubMed: 21656168]
10. Nehls V, Drenckhahn D. Heterogeneity of microvascular pericytes for smooth muscle type alpha-actin. J Cell Biol. 1991; 113:147–154. [PubMed: 2007619]
11. Newcomb PM, Herman IM. Pericyte growth and contractile phenotype: modulation by endothelial-synthesized matrix and comparison with aortic smooth muscle. J Cell Physiol. 1993; 155:385–393. [PubMed: 8482730]
12. Verbeek MM, Otte-Höller I, Wesseling P, Ruiter DJ, de Waal RM. Induction of alpha-smooth muscle actin expression in cultured human brain pericytes by transforming growth factor-beta 1. Am J Pathol. 1994; 144:372–382. [PubMed: 8311120]
13. Attwell D, Mishra A, Hall CN, O'Farrell FM, Dalkara T. What is a pericyte? J Cereb Blood Flow Metab. 2016; 36:451–455. [PubMed: 26661200]
14. Boado RJ, Pardridge WM. Differential expression of alpha-actin mRNA and immunoreactive protein in brain microvascular pericytes and smooth muscle cells. J Neurosci Res. 1994; 39:430–435. [PubMed: 7884822]
15. Daschil N, Obermair GJ, Flucher BE, Stefanova N, Hutter-Paier B, Windisch M, Humpel C, Marksteiner J. CaV1.2 calcium channel expression in reactive astrocytes is associated with the formation of amyloid-β plaques in an Alzheimer's disease mouse model. J Alzheimers Dis. 2013; 37:439–451. [PubMed: 23948887]
16. Hohsfield LA, Daschil N, Orädd G, Strömberg I, Humpel C. Vascular pathology of 20-month-old hypercholesterolemia mice in comparison to triple-transgenic and APPSwDI Alzheimer's disease mouse models. Mol Cell Neurosci. 2014; 63:83–95. [PubMed: 25447943]
17. Ullrich C, Daschil N, Humpel C. Organotypic vibrosections: novel whole sagittal brain cultures. J Neurosci Methods. 2011; 201:131–141. [PubMed: 21835204]
18. Hutter-Schmid B, Kniewallner KM, Humpel C. Organotypic brain slice cultures as a model to study angiogenesis of brain vessels. Front Cell Dev Biol. 2015; 3:52. [PubMed: 26389117]
19. Daschil N, Kniewallner KM, Obermair GJ, Hutter-Paier B, Windisch M, Marksteiner J, Humpel C. L-type calcium channel blockers and substance P induce angiogenesis of cortical vessels associated with beta-amyloid plaques in an Alzheimer mouse model. Neurobiol Aging. 2015; 36:1333–1341. [PubMed: 25619662]

20. Ghassemifar R, Schultz GS, Tarnuzzer RW, Salerud G, Franzén LE. Alpha-smooth muscle actin expression in rat and mouse mesenteric wounds after transforming growth factor-beta1 treatment. Wound Repair Regen. 1997; 5:339–347. [PubMed: 16984444]
21. Bergers G, Song S. The role of pericytes in blood-vessel formation and maintenance. Neuro Oncol. 2005; 7:452–464. [PubMed: 16212810]
22. Perrin BJ, Ervasti JM. The actin gene family: function follows isoform. Cytoskeleton (Hoboken). 2010; 67:630–634. [PubMed: 20737541]
23. Vandekerckhove J, Weber K. Mammalian cytoplasmic actins are the products of at least two genes and differ in primary structure in at least 25 identified positions from skeletal muscle actins. Proc Natl Acad Sci U S A. 1978; 75:1106–1110. [PubMed: 274701]
24. Vandekerckhove J, Weber K. The complete amino acid sequence of actins from bovine aorta, bovine heart, bovine fast skeletal muscle, and rabbit slow skeletal muscle. A protein-chemical analysis of muscle actin differentiation. Differentiation. 1979; 14:123–133. [PubMed: 499690]
25. Kumar A, Crawford K, Close L, Madison M, Lorenz J, Doetschman T, Pawlowski S, Duffy J, Neumann J, Robbins J, Boivin GP, et al. Rescue of cardiac alpha-actin-deficient mice by enteric smooth muscle gamma-actin. Proc Natl Acad Sci U S A. 1997; 94:4406–4411. [PubMed: 9114002]
26. Schildmeyer LA, Braun R, Taffet G, Debiasi M, Burns AE, Bradley A, Schwartz RJ. Impaired vascular contractility and blood pressure homeostasis in the smooth muscle alpha-actin null mouse. FASEB J. 2000; 14:2213–2220. [PubMed: 11053242]
27. Crawford K, Flick R, Close L, Shelly D, Paul R, Bove K, Kumar A, Lessard J. Mice lacking skeletal muscle actin show reduced muscle strength and growth deficits and die during the neonatal period. Mol Cell Biol. 2002; 22:5887–5896. [PubMed: 12138199]
28. Ruzicka DL, Schwartz RJ. Sequential activation of alpha-actin genes during avian cardiogenesis: vascular smooth muscle alpha-actin gene transcripts mark the onset of cardiomyocyte differentiation. J Cell Biol. 1998; 107:2575–2586.
29. Rønnov-Jessen L, Petersen OW. A function for filamentous alpha-smooth muscle actin: retardation of motility in fibroblasts. J Cell Biol. 1996; 134:67–80. [PubMed: 8698823]
30. Kawasaki Y, Imaizumi T, Matsuura H, Ohara S, Takano K, Suyama K, Hashimoto K, Nozawa R, Suzuki H, Hosoya M. Renal expression of alpha-smooth muscle actin and c-Met in children with Henoch-Schönlein purpura nephritis. Pediatr Nephrol. 2008; 23:913–919. [PubMed: 18273647]
31. Abd-el-Basset EM, Fedoroff S. Immunolocalization of the alpha isoform of smooth muscle actin in mouse astroglia in cultures. Neurosci Lett. 1991; 125:117–120. [PubMed: 1881588]
32. Lecain E, Alliot F, Laine MC, Calas B, Pessac B. Alpha isoform of smooth muscle actin is expressed in astrocytes in vitro and in vivo. J Neurosci Res. 1991; 28:601–606. [PubMed: 1870159]
33. Buniatian GH, Gebhardt R, Mecke D, Traub P, Wiesinger H. Common myofibroblastic features of newborn rat astrocytes and cirrhotic rat liver stellate cells in early cultures and in vivo. Neurochem Int. 1999; 35:317–327. [PubMed: 10482352]
34. Abd-el-Basset EM, Fedoroff S. Upregulation of F-actin and alpha-actinin in reactive astrocytes. J Neurosci Res. 1997; 49:608–616. [PubMed: 9302082]
35. Kálmán M, Szabó A. Immunohistochemical investigation of actin-anchoring proteins vinculin, talin and paxillin in rat brain following lesion: a moderate reaction, confined to the astroglia of brain tracts. Exp Brain Res. 2001; 139:426–434. [PubMed: 11534866]
36. Boukhelifa M, Hwang SJ, Valtschanoff JG, Meeker RB, Rustioni A, Otey CA. A critical role for palladin in astrocyte morphology and response to injury. Mol Cell Neurosci. 2003; 23:661–668. [PubMed: 12932445]
37. Moreels M, Vandenabeele F, Dumont D, Robben J, Lambrichts I. Alpha-smooth muscle actin (alpha-SMA) and nestin expression in reactive astrocytes in multiple sclerosis lesions: potential regulatory role of transforming growth factor-beta 1 (TGF-beta1). Neuropathol Appl Neurobiol. 2008; 34:532–546. [PubMed: 18005096]
38. Boado RJ, Pardridge WM. Molecular cloning of the bovine blood-brain barrier glucose transporter cDNA and demonstration of phylogenetic conservation of the 5'-untranslated region. Mol Cell Neurosci. 1990; 1:224–232. [PubMed: 19912773]

39. Zlokovic BV. Neurovascular mechanisms of Alzheimer's neurodegeneration. Trends Neurosci. 2005; 28:202–208. [PubMed: 15808355]
40. Zipser BD, Johanson CE, Gonzalez L, Berzin TM, Tavares R, Hulette CM, Vitek MP, Hovanesian V, Stopa EG. Microvascular injury and blood-brain barrier leakage in Alzheimer's disease. Neurobiol Aging. 2007; 28:977–986. [PubMed: 16782234]
41. Zlokovic B. The Blood-Brain Barrier in Health and Chronic Neurodegenerative Disorders. Neuron. 2008; 57:178–20. [PubMed: 18215617]
42. Ervin JF, Pannell C, Szymanski M, Welsh-Bohmer K, Schmechel DE, Hulette CM. Vascular smooth muscle actin is reduced in Alzheimer disease brain: a quantitative analysis. J Neuropathol Exp Neurol. 2004; 63:735–741. [PubMed: 15290898]
43. Stopa EG, Butala P, Salloway S, Johanson CE, Gonzalez L, Tavares R, Hovanesian V, Hulette CM, Vitek MP, Cohen RA. Cerebral cortical arteriolar angiopathy, vascular beta-amyloid, smooth muscle actin, Braak stage, and APOE genotype. Stroke. 2008; 39:814–21. [PubMed: 18258839]
44. Hulette CM, Ervin JF, Edmonds Y, Antoine S, Stewart N, Szymanski MH, Hayden KM, Pieper CF, Burke JR, Welsh-Bohmer KA. Cerebrovascular smooth muscle actin is increased in nondemented subjects with frequent senile plaques at autopsy: implications for the pathogenesis of Alzheimer disease. J Neuropathol Exp Neurol. 2009; 68:417–424. [PubMed: 19287310]
45. Dore-Duffy PKA, Wang X, Van Buren E. CNS microvascular pericytes exhibit multipotential stem cell activity. J Cereb Blood Flow Metab. 2006; 26:613–624. [PubMed: 16421511]
46. Skalli O, Ropraz P, Trzeciak A, Benzonana G, Gillessen D, Gabbiani G. A monoclonal antibody against alpha-smooth muscle actin: a new probe for smooth muscle differentiation. J Cell Biol. 1986; 3:2787–2796.
47. Wyss-Coray T, Masliah E, Mallory M, McConlogue L, Johnson-Wood K, Lin C, Mucke L. Amyloidogenic role of cytokine TGF-beta1 in transgenic mice and in Alzheimer's disease. Nature. 1997; 389:603–606. [PubMed: 9335500]
48. Wyss-Coray T, Lin C, Sanan DA, Mucke L, Masliah E. Chronic overproduction of transforming growth factor-beta1 by astrocytes promotes Alzheimer's disease-like microvascular degeneration in transgenic mice. Am J Pathol. 2000; 156:139–150. [PubMed: 10623661]
49. Grammas P, Ovase R. Cerebrovascular transforming growth factor-beta contributes to inflammation in the Alzheimer's disease brain. Am J Pathol. 2002; 160:1583–1587. [PubMed: 12000710]
50. Tarkowski E, Issa R, Sjögren M, Wallin A, Blennow K, Tarkowski A, Kumar P. Increased intrathecal levels of the angiogenic factors VEGF and TGF-beta in Alzheimer's disease and vascular dementia. Neurobiol Aging. 2002; 23:237–243. [PubMed: 11804709]
51. Tong XK, Nicolakakis N, Kocharyan A, Hamel E. Vascular remodeling versus amyloid beta-induced oxidative stress in the cerebrovascular dysfunctions associated with Alzheimer's disease. J Neurosci. 2005; 25:11165–11174. [PubMed: 16319316]
52. Ongali B, Nicolakakis N, Lecrux C, Aboulkassim T, Rosa-Neto P, Papadopoulos P, Tong XK, Hamel E. Transgenic mice overexpressing APP and transforming growth factor-beta1 feature cognitive and vascular hallmarks of Alzheimer's disease. Am J Pathol. 2013; 177:3071–3080.
53. Town T, Laouar Y, Pittenger C, Mori T, Szekely CA, Tan J, Duman RS, Flavell RA. Blocking TGF-beta-Smad2/3 innate immune signaling mitigates Alzheimer-like pathology. Nat Med. 2008; 14:681–687. [PubMed: 18516051]
54. Mocali A, Cedrola S, Della Malva N, Bontempelli M, Mitidieri VA, Bavazzano A, Comolli R, Paoletti F, La Porta CA. Increased plasma levels of soluble CD40, together with the decrease of TGF beta 1, as possible differential markers of Alzheimer disease. Exp Gerontol. 2004; 39:1555–1561. [PubMed: 15501026]
55. Juraskova B, Andrys C, Holmerova I, Solichova D, Hrnciarikova D, Vankova H, Vasatko T, Krejsek J. Transforming growth factor beta and soluble endoglin in the healthy senior and in Alzheimer's disease patients. J Nutr Health Aging. 2010; 14:758–761. [PubMed: 21085906]
56. Grammas P. Neurovascular dysfunction, inflammation and endothelial activation: implications for the pathogenesis of Alzheimer's disease. J Neuroinflammation. 2011; 8:26. [PubMed: 21439035]
57. Glass CK, Saijo K, Winner B, Marchetto MC, Gage FH. Mechanisms underlying inflammation in neurodegeneration. Cell. 2010; 140:918–934. [PubMed: 20303880]

58. Blobe GC, Schiemann WP, Lodish HF. Role of transforming growth factor beta in human disease. N Engl J Med. 2000; 342:1350–1358. [PubMed: 10793168]

59. Burton T, Liang B, Dibrov A, Amara F. Transforming growth factor-beta-induced transcription of the Alzheimer beta-amyloid precursor protein gene involves interaction between the CTCF-complex and Smads. Biochem Biophys Res Commun. 2002; 295:713–723. [PubMed: 12099698]

60. Wyss-Coray T, Lin C, Yan F, Yu GQ, Rohde M, McConlogue L, Masliah E, Mucke L. TGF-beta1 promotes microglial amyloid-beta clearance and reduces plaque burden in transgenic mice. Nat Med. 2001; 7:612–618. [PubMed: 11329064]

Europe PMC Funders Author Manuscripts

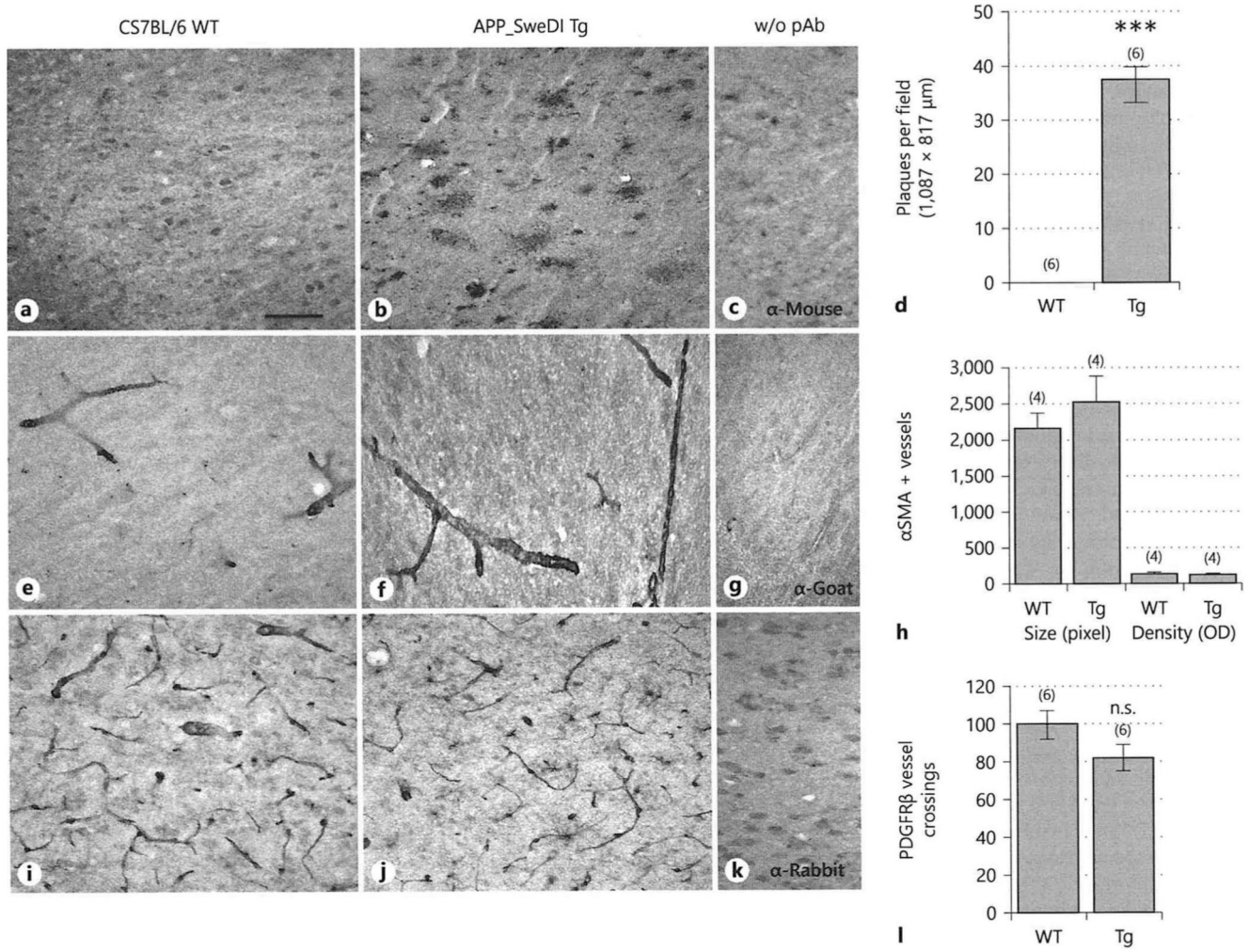

Fig. 1.

Immunohistochemical characterization of 12-month old wildtype (C57BL/6N) and transgenic (Tg-SweDI) mouse brains stained against β-amyloid (Aβ) (A-C), alpha-smooth muscle actin (αSMA) (E-G) and platelet-derived growth factor receptor-beta (PDGFRβ) (I-K). Mice were transcardially perfused with PBS, fresh frozen and 40 µm thick sections were stained with primary antibodies or without (w/o Ab) as a negative control (C-G-K). Staining was visualized by diaminobenzidine. Semi-quantitative analyses for Aβ (D), αSMA (H) or PDGFRβ (L) were performed by counting plaques per field (D), measuring optical density (H) or counting the vessel crossings per field (K). Values are given as mean±SEM. The number of n is given in parenthesis. Statistical analysis was performed by One way ANOVA with a subsequent Fisher LSD posthoc test (*** $p<0.001$, ns, not significant). Scale bar in A= 100 µm (A-C, E-G, I-K).

Europe PMC Funders Author Manuscripts

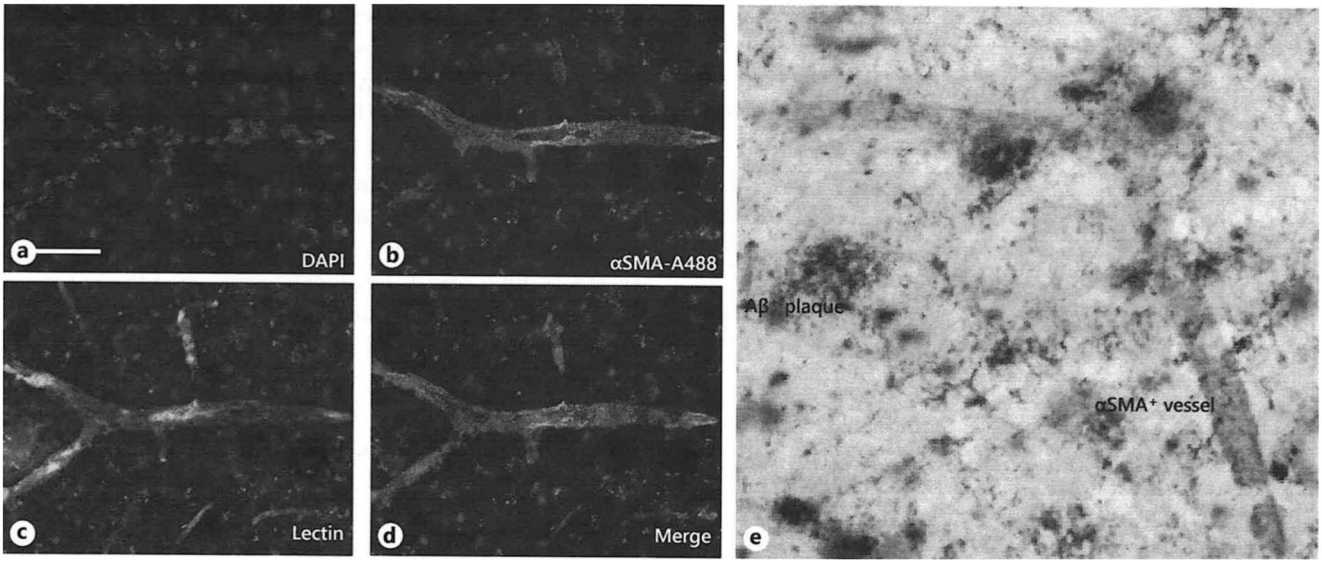

Fig. 2.

Co-localization of alpha-smooth muscle actin (αSMA) with vessel-lectin (C) and β-amyloid (Aβ) (E). Transgenic mice (Tg-SweDI) were transcardially perfused with PBS, fresh frozen and 40 μm thick sections were stained for nuclear DAPI (blue, A), αSMA (Alexa-488, green, B, E), lectin (red, C) and Aβ (E). Staining was visualized by fluorescence (A-D) or chromogenic diaminobenzidine (brown) /SG (grey) (E). Scale bar in A= 25 μm (A-D), 50 μl (E)

Europe PMC Funders Author Manuscripts

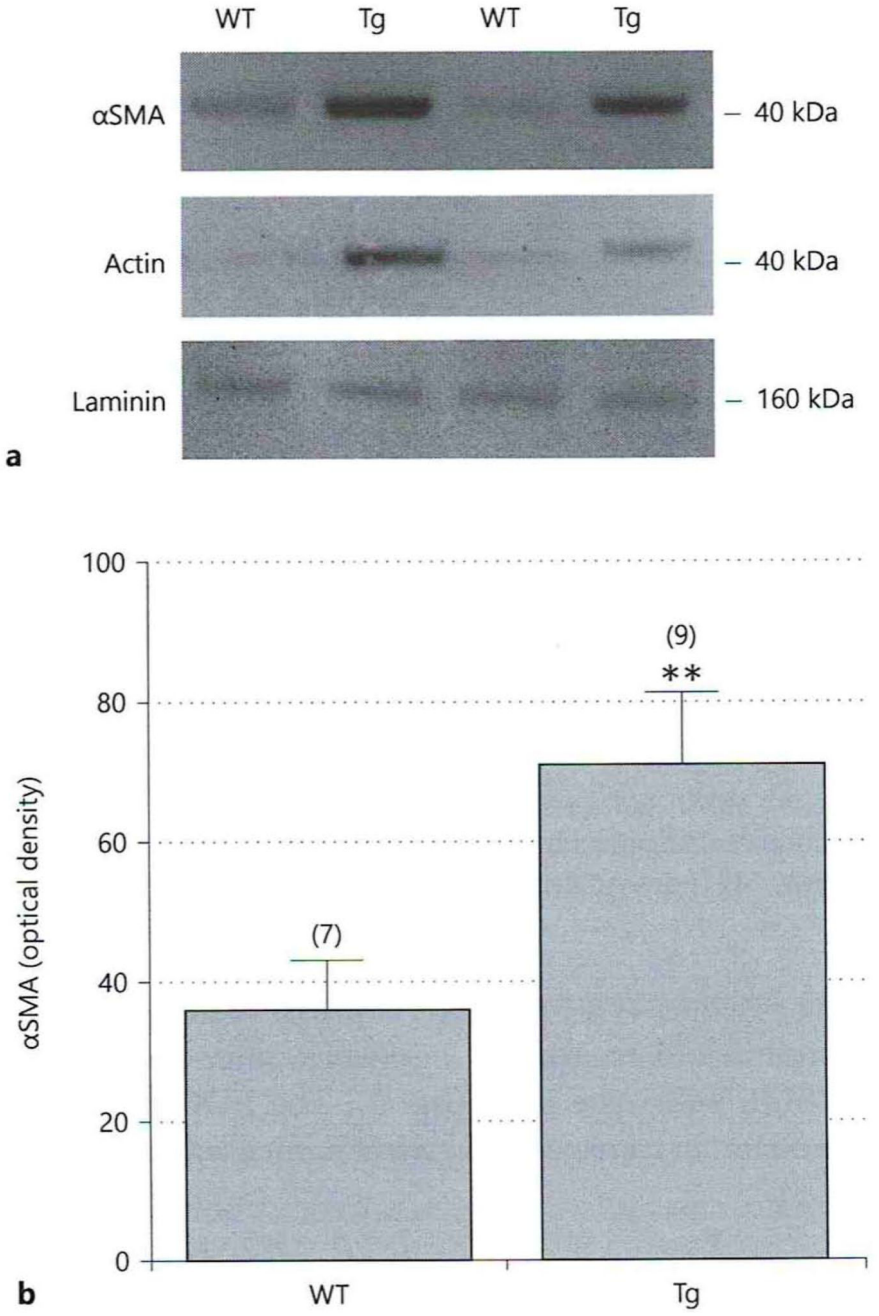

Fig. 3.

Western Blot analysis of cortex vessel extracts isolated from adult 12-month-old wildtype (C57BL/6) and transgenic (Tg-SweDI) mice. Extracted isolated cortex vessel extracts were run on a gel, blotted and then stained with antibodies against alpha-smooth muscle actin (αSMA), actin or laminin (as a loading control). Size markers are given on the right in kDa. αSMA-like immunoreactivity was quantified (optical density) and is given as mean±SEM) (B). Statistical analysis was performed by students T-test (** $p<0.01$). The number of n is given in parenthesis.

Europe PMC Funders Author Manuscripts

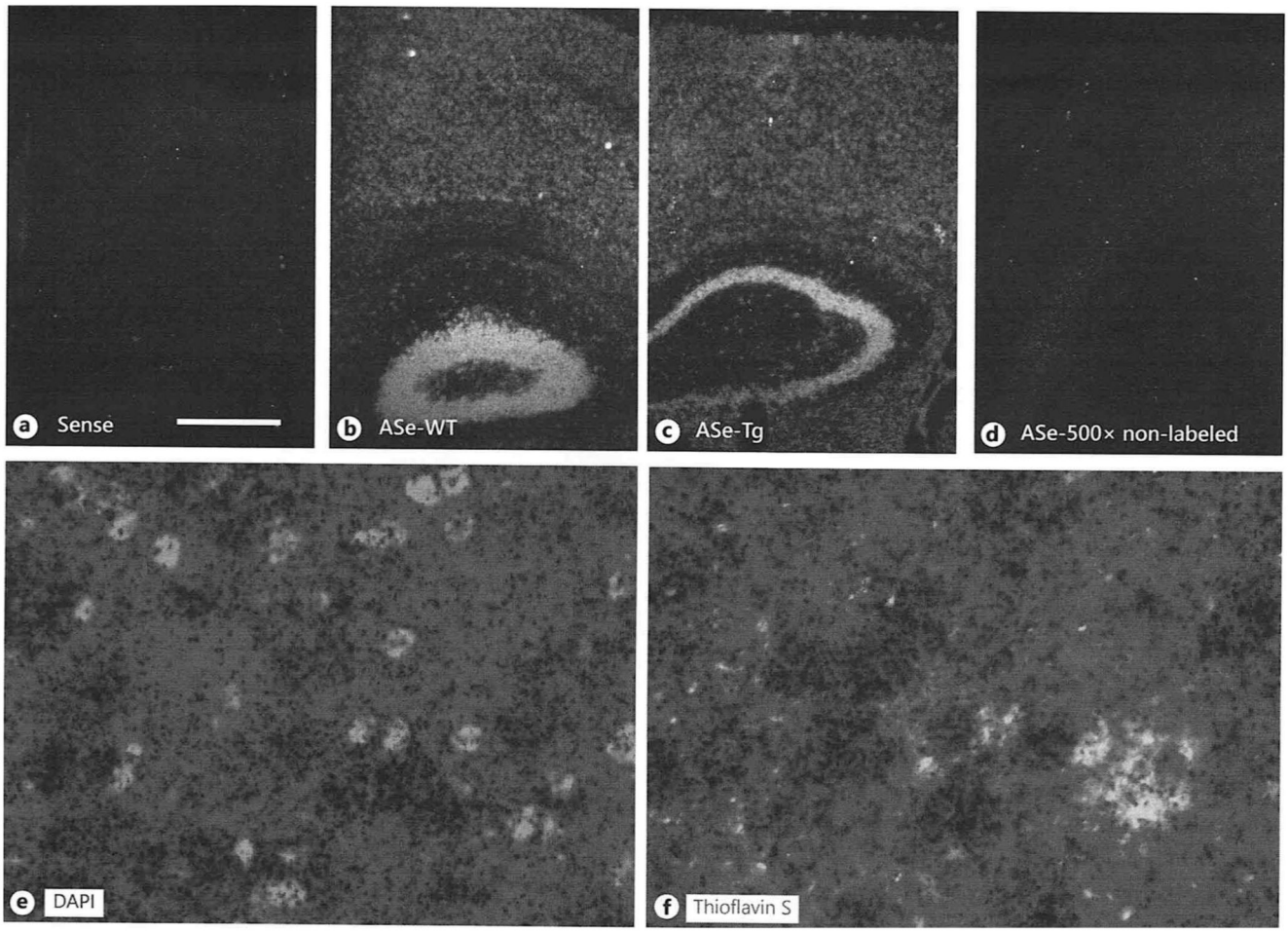

Fig. 4.

In situ hybridization for alpha-smooth muscle actin (αSMA) in 12-month-old wildtype (wt) and transgenic (tg) mice. Brains were fresh frozen, sectioned and labelled with 35S-oligonucleotides and then covered with a film emulsion. Sections were then counterstained with DAPI (E) or thioflavin S to visualize plaques (F). The sense (A) as well as the 500x unlabeled (ASe-500x D) oligonucleotides revealed only background labelling. αSMA antisense oligonucleotides detected αSMA $mRNA^{+}$ cells in cortices and hippocampus of wildtype mice (B) and transgenic (C) mice. Pictures are given as darkfield images showing white silver grains. Note enhanced silver grain densities in the vincinity of thioflavin S stained plaques (F). Scale bar in A = 300 μm (A-D), 29 μm (E-F).

Europe PMC Funders Author Manuscripts

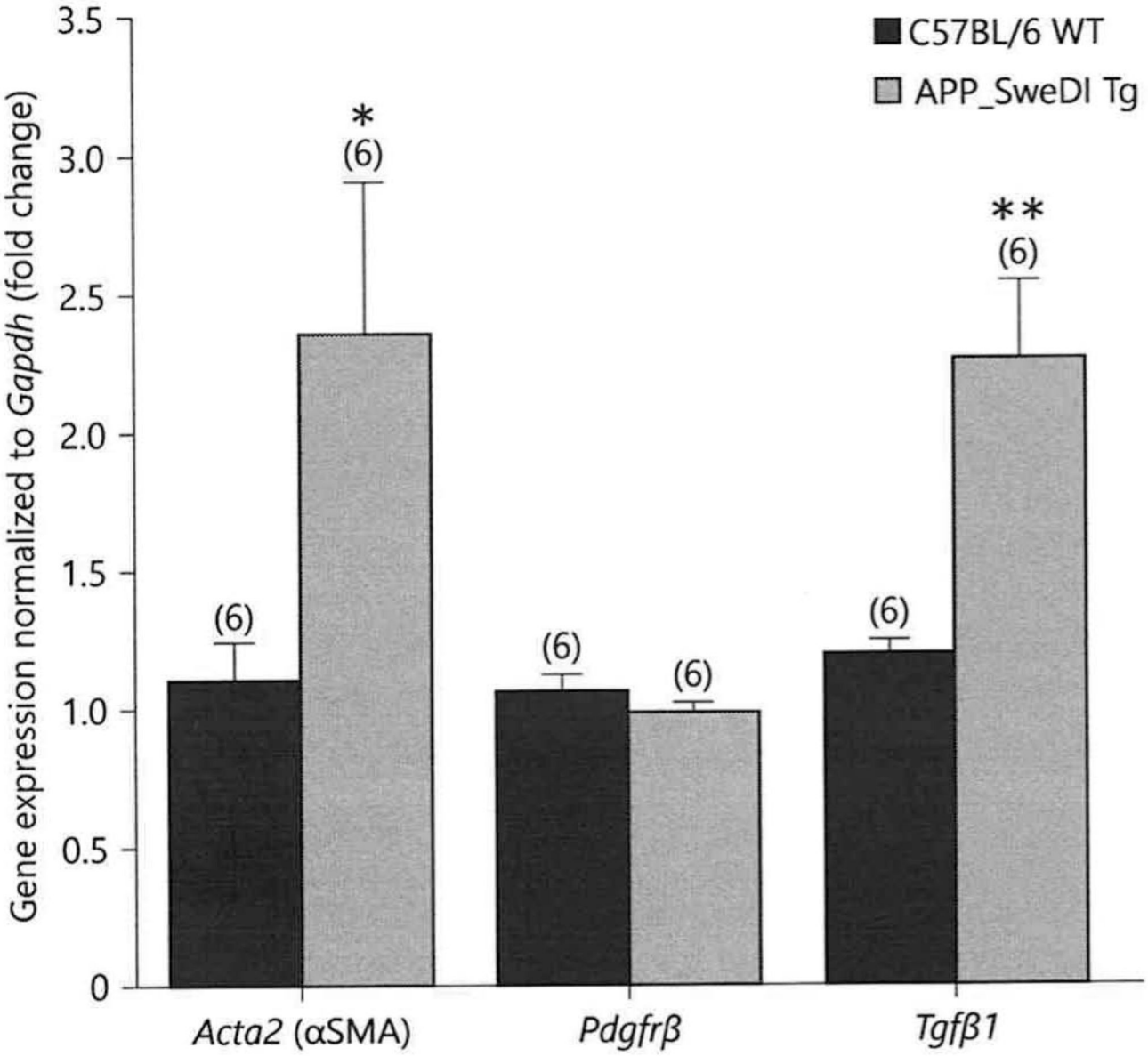

Fig. 5.

Quantitative real-time PCR expression of alpha-smooth muscle actin (αSMA, *Acta2 gene*), transforming growth factor beta-1 (*Tgfβ1*) and platelet-derived growth factor-β (*Pdgfrβ*) in wildtype C57BL/6 and transgenic (Tg-SweDI) mice. mRNA expression of *αSMA, Tgfβ1* and *Pdgfrβ* was determined by isolating mouse brain cortices from 12-month old wildtype C57BL/6 (blue) as well as transgenic (Tg-SweDI) (red) mice. Values are given as means ± SEM normalized to *Gapdh*. The number of n is given in parenthesis. Statistical analysis was performed by students T-test (* $p < 0.05$, ** $p < 0.01$).